Characterization of the Binding Sites for ^{123}I-ADAM and the Relationship to the Serotonin Transporter in Rat and Mouse Brains Using Quantitative Autoradiography

Kun-Ju Lin, MD[1,2]; Tzu-Chen Yen, MD, PhD[2]; Shiaw-Pyng Wey, PhD[3]; Jeng-Jong Hwang, PhD[4]; Xin-Xian Ye, MS[4]; Kai-Yuan Tzen, MD, MS[2]; Ying-Kai Fu, PhD[5]; and Jin-Chung Chen, PhD[6]

[1]Graduate Institute of Clinical Medical Sciences, Chang-Gung University, Tao-Yuan, Taiwan; [2]Department of Nuclear Medicine, Chang-Gung Memorial Hospital, Tao-Yuan, Taiwan; [3]Division of Radiological Technology, School of Medical Technology, Chang-Gung University, Tao-Yuan, Taiwan; [4]Department of Medical Radiation Technology and Institute of Radiological Sciences, National Yang-Ming University, Taipei, Taiwan; [5]Institute of Nuclear Energy Research, Tao-Yuan, Taiwan; and [6]Department of Pharmacology, Chang-Gung University, Tao-Yuan, Taiwan

Imaging of serotonin transporter (SERT) in the central nervous system may provide an important tool to evaluate some psychiatric disorders. Recently, a novel ^{123}I-labeled radiotracer, 2-((2-((dimethylamino)methyl)phenyl)thio)-5-iodophenylamine (^{123}I-ADAM), has been developed that exhibited a high selectivity for SERT. The aim of this study was to characterize the biodistribution and specificity of ^{123}I-ADAM to SERT using quantitative autoradiography in both control and neurotoxin-treated animals. **Methods:** ^{123}I-ADAM (74 MBq) was injected intravenously into the mice to access its biodistribution in the brain via quantitative autoradiography. Further, rats with serotonin depleted by intraperitoneal injection of p-chloroamphetamine (PCA) were used to evaluate the specificity of ^{123}I-ADAM to SERT. The levels of biogenic amines were then measured and correlated with quantitative ^{123}I-ADAM labeling in control and PCA-treated rat brains. **Results:** The autoradiographic results showed that ^{123}I-ADAM accumulated in SERT-rich brain areas after systemic injection, including the globus pallidus, thalamus, hypothalamus, substantia nigra, interpeduncular nucleus, amygdala, and raphe nucleus. The dorsal raphe nucleus had the highest initial uptake with a peak specific binding ratio (i.e., [target − cerebellum]/cerebellum) at 120 min after injection. ^{123}I-ADAM uptake was dramatically decreased in the hippocampus, thalamus, amygdala, geniculate nuclei, hypothalamus, raphe nucleus, and substantia nigra in PCA-lesioned rats. The decrement in radioactivity was more prominent at higher dosages of PCA and was in parallel with the changes in amounts of serotonin and 5-hydroxyindoleacetic acid in the prefrontal cortex. **Conclusion:** This study demonstrates that regional distribution of ^{123}I-ADAM radioactivity is similar to the SERT localization in both rat and mouse brains. We also validated that destruction on central serotonergic neurons after PCA treatment inhibits the uptake of ^{123}I-ADAM in serotonin-rich brain regions. High specific binding to SERT in vivo makes ^{123}I-ADAM an appropriate radiotracer for solitary studies of serotonin functions in living humans.

Key Words: quantitative autoradiography; serotonin transporter; biodistribution

Aberrant serotonergic function plays an important role in the pathogenesis of psychiatric disorders (1). However, only a few neurochemical imaging studies using PET or SPECT have been performed because of difficulties in the selection of a suitable selective radiotracer for in vivo clinical assessment (2). Due to the high nonspecific binding to other neurotransmitter transporters as well as difficulties in radiolabeling, only a few radiotracers are used in daily clinical practice.

Recently, a promising novel iodinated SPECT tracer, 2-((2-((dimethylamino)methyl)phenyl)thio)-5-iodophenylamine (ADAM), has been developed (3,4). ADAM showed a >1,000-fold selectivity for the serotonin transporter (SERT) over the norepinephrine transporter (NET) and the dopamine transporter (DAT) (inhibition constant = 699 and 840 nmol/L for NET and DAT, respectively) (4). The relatively longer radioactivity half-life of this ^{123}I-labeled compound makes it more convenient to prepare and image than the ^{11}C-labeled tracers. Recently, quantification of SERT in baboon brain by this novel drug has been reported using full kinetic modeling, which showed a specific binding ratio (i.e., [target − cerebellum]/cerebellum) of 2.16 in the midbrain (5). These data suggest that the new radioligand ^{123}I-ADAM would be applicable to SPECT imaging of the SERT binding sites in the human brain.

The biodistribution of this novel drug has been recently established in both animals and humans (5–7). These data were calculated based on the radioactivity distribution collected either using tissue dissection or planar image acquisition methods (6,7). However, the SERT is diffusely and heterogeneously distributed in the brain (8), which makes discrimination of brain regions via conventional methods unsatisfactory. Besides, the specificity of this novel drug has not been well studied. Quantitative autoradiography is a useful technique to demonstrate the distribution of the tracer in the brain with high resolution (9). The recent advance of radioluminography using phosphor-imaging plate (IP) has enabled the quantification of radioactivity expressed as the intensity of photostimulated-luminescence (PSL) over a wide range (10,11). We report the biodistribution of this novel drug in detail using ex vivo quantitative autoradiography with IP. To further evaluate its specificity to SERT, ^{123}I-ADAM distribution among different brain nuclei in normal and p-chloroamphetamine (PCA)-treated rats was also determined.

MATERIALS AND METHODS

Radiotracer

^{123}I-ADAM with high specific activity (>444 TBq/mmol [>12,000 Ci/mmol]) was prepared by an oxidative iododestannylation reaction that was modified from a procedure reported elsewhere (3,4). Briefly, 100 μg of a tin precursor, 2-((2-((dimethylamino)methyl)phenyl)thio)-5-(tri-n-butyltin)phenylamine, was reacted with approximately 5.55 GBq ^{123}I-NaI (Institute of Nuclear Energy Research) in the presence of hydrogen peroxide and diluted acetic acid for 5 min. After quenching with NaHSO$_3$, the neutralized reaction mixture was loaded onto an octyl cartridge (Accubond; J&W Scientific) for purification. The cartridge was washed with water and 50% ethanol to remove impurities. Purified ^{123}I-ADAM was obtained by eluting the cartridge with absolute ethanol, and it was diluted further with 0.9% saline for the animal studies. The radiochemical purity determined by high-performance liquid chromatography (HPLC) was normally >90%.

Animals

Four-week-old male ICR mice weighing 15–20 g were used in the pharmacokinetic study. Male Sprague–Dawley rats (200–250 g) were used in the biodistribution and PCA treatment studies. The animals were kept on a complete pellet diet (Lab Diet), at a room temperature of 25°C, and on a light:dark cycle of 12:12 h (lights on at 07:00 AM), with free access to tap water. The animals were allowed to acclimate to this environment for a period of 2 wk before the beginning of the experiments. The animal experiments were approved by the Laboratory Animal Care Panel of the National Yang Ming University and Chang Gung University.

Biodistribution of ^{123}I-ADAM in Mouse Brain

In the first series of experiments, 18 mice were given 74 MBq ^{123}I-ADAM through the tail vein. The animals were killed with chloroform at 30, 60, 90, 120, 240, and 360 min after drug injection (n = 3 at each time point). The brains were rapidly removed, placed in embedding medium, and frozen immediately with dry ice. After equilibrium at −20°C, consecutive 20-μm coronal sections were cut with a Bright OTF cryomicrotome and thaw-mounted onto microscope slides. The slides containing the brain sections were dried in air at room temperature and stored for further processing.

Levels of Biogenic Amines and Metabolites in Prefrontal Cortex of PCA-Treated and Control Rats

In the second series of experiments, levels of biogenic amine in the prefrontal cortex were examined in both PCA-treated and control rats (n = 5–8 in each group). The rats were killed by decapitation and the brain was rapidly removed. The prefrontal cortex was dissected and homogenized for 15 s with an ultrasonic cell disruptor in 200 μL of ice-cold 0.1 mol/L perchloric acid. The homogenates were centrifuged at 19,100g for 30 min at 4°C, and the supernatants were filtered through a 0.2-μm filter. These filtrates were then injected into an HPLC system. The HPLC system (model 125; Beckman) consisted of a solvent delivery pump, an analytic C$_{18}$ reversed-phase column (5-μm ODS; 3 × 10 cm; Beckman), and an electrochemical detector (LC-4C; BAS Inc.). Aliquots (10 μL) of the filtrates were injected onto a C$_{18}$ reversed-phase column, eluted with a citrate-base mobile phase (30 mmol/L citric acid buffer [pH 4.6] containing 50 mmol/L sodium acetate, 5.2 mmol/L sodium hydroxide, and 18.3 mmol/L 1-octanesulfonic acid in 9% methanol) at a flow rate of 1 mL/min and a temperature of 25°C. The separated monoamines and metabolites were measured with an electrochemical detector with an oxidation potential setting at +0.65 V. The concentration of each compound in the brain samples was calculated by comparison with external standards, injected every 5 sample runs.

Biodistribution of ^{123}I-ADAM in PCA-Treated and Control Rat Brain

In the third experiment, 12 Sprague–Dawley rats were divided into 4 treatment groups: saline, PCA (2 mg/kg, intraperitoneally), PCA (5 mg/kg, intraperitoneally), and PCA (10 mg/kg, intraperitoneally). Seven days after drug treatment, the animals were sacrificed with chloroform 2 h after the injection of 185 MBq ^{123}I-ADAM. The brains were sectioned as described and stored for further processing. Adjacent Nissl-stained brain sections were prepared for comparison, and the brain regions were identified according to Paxinos and Watson's atlas of the rat brain (12).

Quantitative Autoradiography

Brain slices prepared from the first and third experiments were then applied to the BAS-SR IP for an autoradiography study.

Two types of standards were prepared. The filter paper standards were made with 3M filter papers (Whatman Inc.) loaded with serial dilutions of ^{123}I-ADAM. A solution of ^{123}I-ADAM was prepared at a concentration of 16 MBq/mL measured with a radioisotope calibrator. The solution was further diluted to 1.97–160 kBq/mL, and 10 μL of each diluted solution (0.0197–1.6 kBq) were loaded onto 5 pairs of filter paper. One set of the dried step-wedge standards made from them was counted in a well scintillation counter. The cpm/Bq was computed with a decay correction. The second set of the filter paper standards was applied to the BAS-SR IP accompanied with the brain sections being studied for 5 d until the complete decay of the [123]I. After the exposure was completed, the cassette was opened under subdued light and the IPs were measured with a FLA-5000 IP reader (Fuji Photo Film Co.). The known radioactivities of the applied standards were then correlated with the intensity of PSL of the filter paper standards measured with the bioimage analyzer MacBas version 2.5 (Fuji Photo Film Co.).

The tissue standards were made from serial sections of the rat brain at different levels. To obtain coronal brain sections having a wide range of radioactivities, the ex vivo autoradiography was performed 30 min and 2 h after injection of ^{123}I-ADAM. After killing the animals, 20 pairs of adjacent coronal brain sections through the prefrontal region with a 20-μm thickness were prepared. One set of the brain sections was applied to the IP until the complete decay to measure the PSL for the whole section as described. The adjacent section was counted in a well scintillation counter for radioactivity (cpm) measurement. The known radioactivities of the applied tissue standards were then correlated with the PSL results. Then, the PSL/cpm and PSL/Bq were calculated for each brain section.

Regions of interest were placed on the prefrontal cortex, globus pallidus, hypothalamus, substantia nigra, raphe nuclei, and cerebellum corresponding to the stereotactic atlas to measure the regional brain volume (mm² × 0.02 mm), which was converted to Bq/mL. Then, the uptake of ^{123}I-ADAM was assessed as the percentage of injected dose per milliliter of tissue (%ID/mL). The specific binding was expressed as the ratios of (targets – cerebellum) to the cerebellum.

RESULTS

Calibration of PSL

The solid circles in Figure 1 represent the relationship between PSL and the radioactivities of the filter paper standards. The PSL values displayed a linear relationship to the ^{123}I-ADAM radioactivities measured with a well-type γ-counter, and the ratio was 2.43 PSL/cpm at the start of the contact. The linearity between the dose calibrator and the well-type γ-counter was also calculated, and this ratio was 35 cpm/Bq. Since the radioactivities loaded on the filter

FIGURE 1. Relationship between PSL values and ^{123}I-ADAM radioactivities on filter standards and tissue standards obtained from 20-μm-thick sections of prefrontal cortex.

papers were uniformly distributed, the PSL of the filter paper standards thus could be translated as a linear function of radioactivities in the range from 0.04 to 104 Bq/mm² with the ratio of 85 PSL/Bq.

The open circles in Figure 1 represent the relationship between PSL and the ^{123}I-ADAM radioactivities of tissue standards obtained from 20-μm sections of the prefrontal cortex. The PSL values also displayed a linear relationship to the radioactivities within the tissue standards. However, the ratio was different between the 2 standards. The PSL of the tissue standards could be translated as a linear function of the radioactivities in the range from 0.04 to 10 Bq/mm², and the ratio was 426.3 PSL/Bq.

Biodistribution of ^{123}I-ADAM in Mouse and Rat Brains

The mapping of the ^{123}I-ADAM binding sites was performed in both mouse and rat brains using quantitative autoradiography compared with the corresponding tissue standards. Figure 2 shows the biodistribution in the mouse brain at 30, 60, and 120 min after intravenous injection of 74 MBq ^{123}I-ADAM. The autoradiographic illustration shows that the ^{123}I-ADAM was accumulated in SERT-rich areas, including the globus pallidus, thalamus, hypothalamus, substantia nigra, interpeduncular nucleus, amygdala, and raphe nuclei. The uptake of ^{123}I-ADAM in the mouse brain at different time points is listed in Table 1. The dorsal raphe nucleus, median raphe nucleus, and substantia nigra had the highest radioactivities in the testing areas and decreased over prolonged times. On the other hand, the cerebellum had the lowest initial uptake, and its activity decreased to a greater extent 1 h after tracer injection. To estimate the time course of specific binding, the cerebellum was used as the background region. The cerebellar activities were divided from each brain region after subtraction—that is, ([target − cerebellum]/cerebellum) at each time point (Fig. 3). The approximate peak of individual specific binding curve was identified and recorded as the time of transient equilibrium. The specific binding ratio of the hypothalamus and the frontal cortex reach a peak value at 1 h after drug injection and then decreased slowly. The dorsal raphe nucleus had the highest initial uptake with a peak specific binding ratio at 120 min after injection of ^{123}I-ADAM. The substantia nigra had the highest specific binding ratio among all of the testing regions and reached to its maximum value at 240 min after tracer injection. Figure 3 shows that there was a trend of increasing peak equilibrium time with higher specific binding ratio.

The detailed anatomic distribution of the radiotracer in rats is shown in Figure 4, using quantitative autoradiographic analysis. The uptake of ^{123}I-ADAM in different rat brain regions at 2 h after tracer injection is listed in Table 2. The results revealed that the radioactivities were located in profound rat brain regions and were heterogeneously distributed. The high-density regions (%ID/mL, >0.7) were located in the dorsal raphe nucleus, median raphe nucleus, interpeduncular nucleus, substantia nigra, medial forebrain
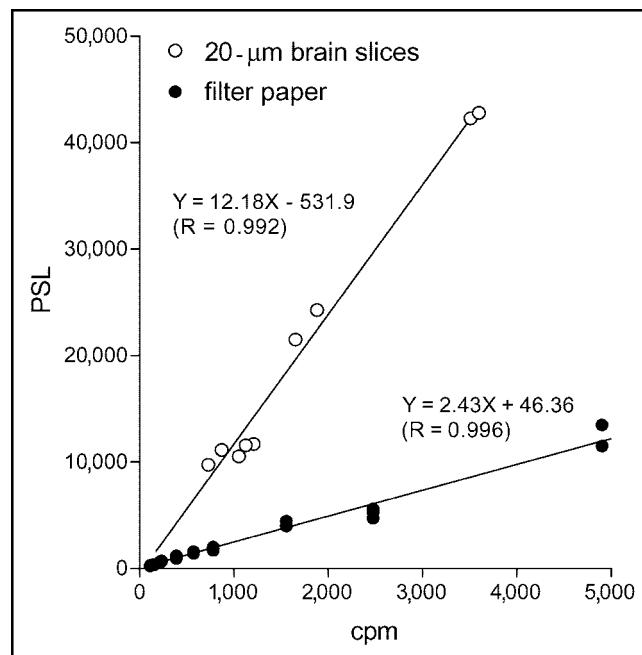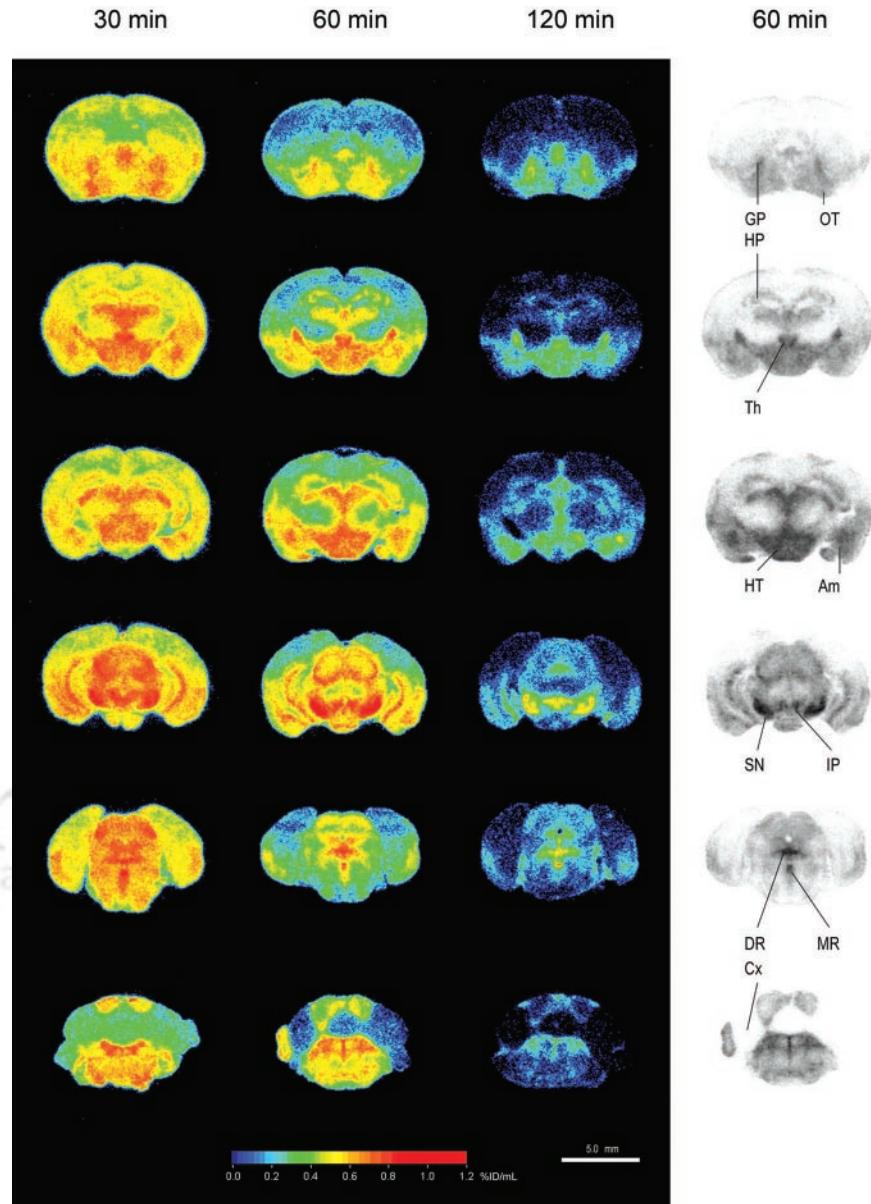
FIGURE 2. Autoradiographic illustration of mouse brain at 30, 60, and 120 min after intravenous injection of 74 MBq ^{123}I-ADAM. Am = amygdala; Cx = cerebellum; DR = dorsal raphe nucleus; GP = globus pallidus; HP = hippocampus; HT = hypothalamus; IP = interpeduncular nucleus; MR = median raphe nucleus; OT = olfactory tubercle; SN = substantia nigra; Th = thalamus.

bundle, nucleus raphe magnus, lateral hypothalamus, ventral lateral geniculate nucleus, globus pallidus, basolateral amygdala, and ventromedial hypothalamus. The moderate-density regions (%ID/mL range, 0.7–0.5) were found in the mediodorsal thalamus, superior colliculus, lateral dorsal thalamus, olfactory tubercle, dorsal hypothalamus, dorsal lateral geniculate nucleus, basomedial amygdala, lateral amygdala, and hippocampus. The low-density regions (%ID/mL, <0.5) were identified in the cingulum, ventral hypothalamus, caudate putamen, ventral pallidum, lateral septal nucleus, prefrontal cortex, and cerebellum. Within the amygdaloid complex, the uptake of ^{123}I-ADAM was detected in different nuclei with differential labeling. The basolateral nuclei had a higher uptake of the radiotracer than the lateral amygdaloid nuclei. In comparison with the adjacent Nissl-stained brain sections, the uptake of ^{123}I-ADAM showed a differential laminar distribution in the hippocampus. The stratum moleculare of the CA1 region had a higher uptake compared with the CA1–CA3 pyramidal cell layer and granule cell layer of the dentate gyrus. The thalamic nuclei also showed a differential uptake of ^{123}I-ADAM that varied from a low density in the ventral nuclei to a moderate to high density in the mediodorsal, laterodorsal, and ventromedial nuclei. A higher density was seen in the lateral nuclei of hypothalamus compared with other regions of the hypothalamus, corresponding to the hypothalamic path of the medial forebrain bundle. The substantia nigra had a higher uptake in its peripheral part than in its central region. The distribution of ^{123}I-ADAM in the rat brain correlated well with SERT immunohistochemistry reported elsewhere (8).

TABLE 1
Biodistribution of ^{123}I-ADAM in Mouse Brain Regions at 30 Minutes to 6 Hours After Intravenous Injection of Radiotracer

Region	Biodistribution (%ID/mL)				
	30 min	60 min	120 min	240 min	360 min
Olf	0.50 ± 0.09	0.43 ± 0.11	0.14 ± 0.03	0.05 ± 0.01	0.03 ± 0.01
GP	0.54 ± 0.02	0.60 ± 0.11	0.33 ± 0.07	0.10 ± 0.01	0.03 ± 0.00
Cortex	0.29 ± 0.01	0.20 ± 0.06	0.09 ± 0.02	0.04 ± 0.00	0.02 ± 0.00
HP	0.47 ± 0.07	0.41 ± 0.07	0.15 ± 0.04	0.05 ± 0.00	0.03 ± 0.00
Th	0.74 ± 0.10	0.70 ± 0.13	0.34 ± 0.07	0.09 ± 0.01	0.03 ± 0.00
HT	0.63 ± 0.10	0.68 ± 0.11	0.33 ± 0.08	0.09 ± 0.01	0.03 ± 0.00
Am	0.55 ± 0.08	0.59 ± 0.10	0.25 ± 0.06	0.07 ± 0.01	0.03 ± 0.00
SN	0.88 ± 0.03	0.97 ± 0.18	0.58 ± 0.09	0.30 ± 0.03	0.11 ± 0.01
IP	0.89 ± 0.02	0.79 ± 0.15	0.46 ± 0.09	0.15 ± 0.00	0.06 ± 0.00
DR	0.91 ± 0.03	0.95 ± 0.14	0.61 ± 0.13	0.19 ± 0.02	0.08 ± 0.00
MR	0.91 ± 0.07	0.85 ± 0.11	0.53 ± 0.10	0.21 ± 0.03	0.06 ± 0.01
ST	0.44 ± 0.08	0.43 ± 0.11	0.14 ± 0.03	0.05 ± 0.00	0.02 ± 0.00
Cx	0.27 ± 0.01	0.13 ± 0.02	0.07 ± 0.01	0.03 ± 0.00	0.02 ± 0.00

Olf = olfactory bulb; GP = globus pallidus; HP = hippocampus; Th = thalamus; HT = hypothalamus; Am = amygdala; SN = substantia nigra; IP = interpeduncular nucleus; DR = dorsal raphe nucleus; MR = median raphe nucleus; ST = striatum; Cx = cerebellum.
Data are expressed as the average of 3 mice ± SD.

Levels of Biogenic Amines and Metabolites and Biodistribution of ^{123}I-ADAM in PCA-Treated and Control Rats

Figure 5 shows the effects of PCA on biogenic amines 7 d after drug treatment. The amounts of serotonin and its major metabolite, 5-hydroxyindoleacetic acid (5-HIAA), in the prefrontal cortices decreased with increasing dosages of PCA. On the other hand, the levels of dopamine and its major metabolite, homovanillic acid (HVA), did not change between PCA-treated and control rats, indicating the specific serotonin toxicity by the treatment of PCA.

The effect of selective lesions on serotonergic neurons by intraperitoneal injection of different dosages of PCA was also examined by ^{123}I-ADAM quantitative autoradiography. The results showed that in PCA-lesioned rats, ^{123}I-ADAM uptake was dramatically decreased in several brain regions (Fig. 6). The specific binding ratio was profoundly deceased in the globus pallidus, dorsal raphe nucleus, median raphe nucleus, hypothalamus, prefrontal cortex, and substantia nigra. Partially reduced specific binding ratio was identified in the medial forebrain bundle and hippocampus. All brain regions exhibited a progressive decline in ^{123}I-ADAM specific binding ratio after a higher dose of PCA treatment. After treatment with the increasing dosages of PCA, the declines of specific binding ratio in different rat brain regions were similar, except in the hippocampus (Fig. 7). The percentage of decline in specific binding ratio at 10 mg/kg PCA varied from >85% in the dorsal raphe nucleus, substantia nigra, globus pallidus, and prefrontal cortex to <55% in hippocampal regions as compared with controls.

DISCUSSION

Autoradiography has several advantages over conventional tissue dissection and analytic methods for evaluating the distribution of radiotracers. This technique can distinguish among the relative concentrations of radioactivity within specific regions of nonhomogeneous organs, allowing detection of potential sites of drug accumulation that are very small, poorly demarcated, or not accessible through macroscopic dissection (6). However, traditional methods using digitalized images of the optical density in the film
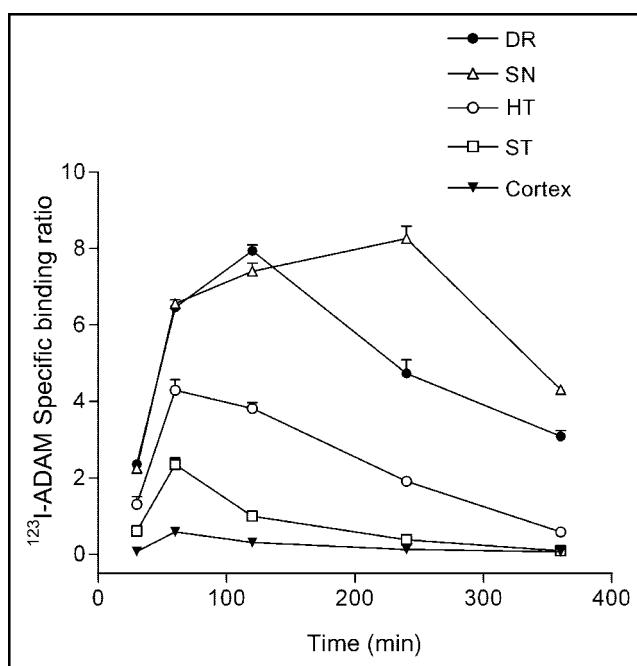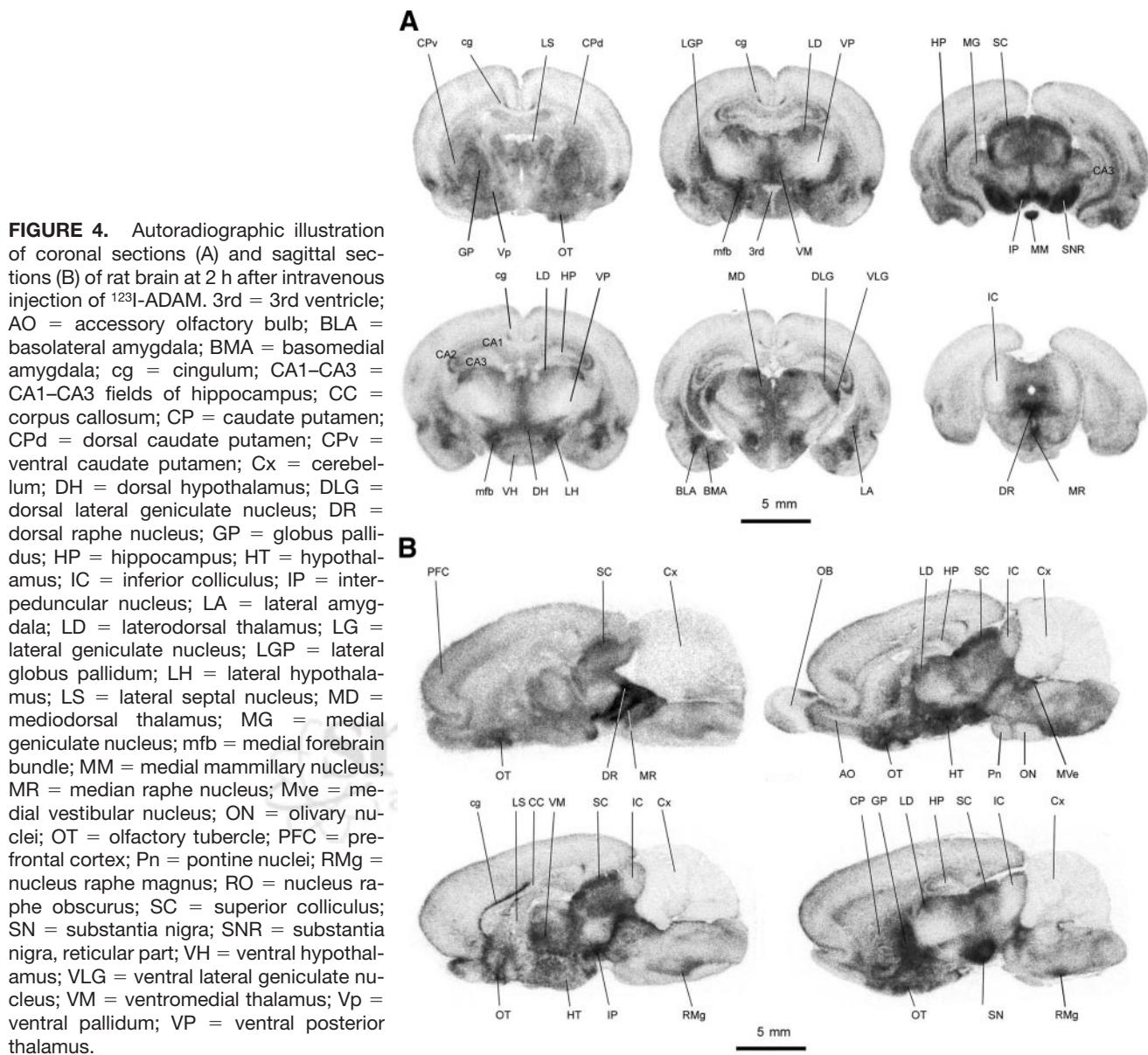

FIGURE 3. Specific binding ratio of ^{123}I-ADAM in brain regions that accumulated a high amount of radiotracer. DR = dorsal raphe nucleus; SN = substantia nigra; HT = hypothalamus; ST = striatum.

FIGURE 4. Autoradiographic illustration of coronal sections (A) and sagittal sections (B) of rat brain at 2 h after intravenous injection of ^{123}I-ADAM. 3rd = 3rd ventricle; AO = accessory olfactory bulb; BLA = basolateral amygdala; BMA = basomedial amygdala; cg = cingulum; CA1–CA3 = CA1–CA3 fields of hippocampus; CC = corpus callosum; CP = caudate putamen; CPd = dorsal caudate putamen; CPv = ventral caudate putamen; Cx = cerebellum; DH = dorsal hypothalamus; DLG = dorsal lateral geniculate nucleus; DR = dorsal raphe nucleus; GP = globus pallidus; HP = hippocampus; HT = hypothalamus; IC = inferior colliculus; IP = interpeduncular nucleus; LA = lateral amygdala; LD = laterodorsal thalamus; LG = lateral geniculate nucleus; LGP = lateral globus pallidum; LH = lateral hypothalamus; LS = lateral septal nucleus; MD = mediodorsal thalamus; MG = medial geniculate nucleus; mfb = medial forebrain bundle; MM = medial mammillary nucleus; MR = median raphe nucleus; Mve = medial vestibular nucleus; ON = olivary nuclei; OT = olfactory tubercle; PFC = prefrontal cortex; Pn = pontine nuclei; RMg = nucleus raphe magnus; RO = nucleus raphe obscurus; SC = superior colliculus; SN = substantia nigra; SNR = substantia nigra, reticular part; VH = ventral hypothalamus; VLG = ventral lateral geniculate nucleus; VM = ventromedial thalamus; Vp = ventral pallidum; VP = ventral posterior thalamus.

limit the reliability of quantitative measurements (*9*). The shortcoming relates to the intrinsic and statistical fluctuations of the standard measurements, the narrow range of usability of the calibration curve due to saturation of the film, and the use of an emulsion for quantifications that is often uncertain—in particular, the fluctuations of the emulsion thickness. With the recent advances in phosphor imaging, higher sensitivity and a wider linear range can be achieved compared with standard autoradiographic films (*13*). In our current results, the linear relationship of radioactivities and PSL values can be made in the range of $0.04–104$ Bq/mm^2 in filter paper standards and $0.04–10$ Bq/mm^2 in tissue standards. The coefficient was different between the 2 standard measurements (i.e., 85 PSL/Bq for filter paper standards and 426.3 PSL/Bq for tissue standards), possibly due to different attenuation effects of the sample thickness. Therefore, the PSL values can be converted into radioactivity expressed as becquerel units, if the radioactivity of the adjacent brain sections with the same thickness is measured with a γ-counter. To simplify the process, we measured the filter paper standards in each experiment and then translated the level to tissue standards according to the known coefficient differences between these 2 methods.

Several approaches have been applied for quantification of transporter or receptor by emission tomography studies (*14*). A simplified method using specific binding at equilibrium as the index of binding potential requires just a single scanning session and makes the imaging protocol more tolerable in a routine clinical environment (*14*). Basically, the conditions for equilibrium are fulfilled at the time point when the number of molecules that dissociate from the

TABLE 2
Biodistribution and Specific Binding Ratio of ^{123}I-ADAM in Rat Brain at 2 Hours After Injection of Radiotracer

Brain region	Biodistribution (%ID/mL)	Specific binding ratio
High density		
Dorsal raphe nucleus	1.28 ± 0.12	16.48 ± 1.62
Median raphe nucleus	1.23 ± 0.23	15.72 ± 3.18
Interpeduncular nucleus	1.04 ± 0.02	13.20 ± 0.33
Substantia nigra (reticular part)	0.97 ± 0.09	12.23 ± 1.27
Medial forebrain bundle	0.94 ± 0.14	11.79 ± 1.94
Nucleus raphe magnus	0.84 ± 0.07	10.47 ± 0.94
Hypothalamus (lateral)	0.84 ± 0.06	10.39 ± 0.80
Geniculate nucleus (ventral lateral)	0.81 ± 0.06	10.08 ± 0.79
Globus pallidus	0.76 ± 0.01	9.31 ± 0.19
Amygdala (basolateral)	0.72 ± 0.06	8.86 ± 0.86
Thalamus (ventromedial)	0.72 ± 0.08	8.76 ± 1.02
Moderate density		
Thalamus (mediodorsal)	0.68 ± 0.01	8.31 ± 0.20
Superior colliculus	0.66 ± 0.04	8.04 ± 0.51
Thalamus (laterodorsal)	0.66 ± 0.08	8.03 ± 1.08
Olfactory tubercle	0.60 ± 0.05	7.18 ± 0.71
Hypothalamus (dorsal)	0.60 ± 0.09	7.12 ± 1.27
Geniculate nucleus (dorsal lateral)	0.57 ± 0.03	6.77 ± 0.35
Amygdala (basomedial)	0.55 ± 0.02	6.46 ± 0.22
Amygdala (lateral)	0.55 ± 0.04	6.44 ± 0.54
Hippocampus	0.51 ± 0.07	5.95 ± 0.91
Low density		
Cingulum	0.46 ± 0.03	5.29 ± 0.39
Hypothalamus (ventral)	0.43 ± 0.04	4.82 ± 0.48
Caudate putamen (dorsal)	0.35 ± 0.01	3.74 ± 1.68
Ventral pallidum	0.33 ± 0.25	3.49 ± 3.40
Lateral septal nucleus	0.32 ± 0.17	3.30 ± 0.47
Caudate putamen (ventral)	0.29 ± 0.05	2.96 ± 2.35
Prefrontal cortex	0.25 ± 0.06	2.38 ± 0.85
Cerebellum	0.07 ± 0.00	Reference

SERT is equivalent to the number that associate with them (14). According to the specific binding curve obtained from quantitative autoradiography, the transient equilibrium in the dorsal raphe was reached 120 min after tracer administrated in mice, with a specific binding ratio of 7.94 ± 0.26. These results are comparable with the report from Choi et al. (3). However, the time at which equilibrium occurs may change among different brain regions due to the density of available SERT. As shown in our results, the peak specific binding ratio of ^{123}I-ADAM in the substantia nigra was 14 times higher than that of the cortex (8.26 vs. 0.59) but reached to its equilibrium at later time as compared with the cortex (240 vs. 60 min).

The SERT is a member of the neurotransmitter transporter superfamily that mediates the Na^+-dependent uptake of serotonin (15). SERT, as measured by serotonin uptake, radioligand binding, or immunocytochemistry, has been found throughout the brain, reflecting a widespread innervation by serotonin-containing neurons. Our results that showed distribution of ^{123}I-ADAM in various mouse and rat brain regions via autoradiography are in agreement with previous results (3,8). In addition, the amount of ^{123}I-ADAM specific binding ratio in different rat brain regions correlates well with the SERT density, making it a useful radiotracer for SERT detection and quantification (8). As compared with other SERT-rich areas, the ^{123}I-ADAM specific binding ratio in the prefrontal cortex was relatively low (0.59 in mice and 2.38 in rats). Although SERT-like immunoreactivity can be homogenously found in this area, the low density due to the sparse innervation by serotonergic neurons makes it difficult to detect by autoradiography (8). Given the importance of the cortical serotonin function in psychiatric diseases, such as major depression and biopolar disorder, efforts should be made to maximize the sensitivity in detecting the changes of SERT density (1). According to the time–activity curve of the biodistribution result, acquiring the image at an earlier equilibrium time that could optimize the cortical SERT binding may be helpful.

PCA is a useful pharmacologic tool for selective depletion of brain serotonin, damaging serotonin-containing nerve fibers (decreased SERT binding), and producing hyporeactivity in rats as reported previously (16,17) and also observed in the current study (data not shown). As expected, the amount of serotonin and 5-HIAA and the amount of ^{123}I-ADAM–labeled SERT in the prefrontal cortex were concomitantly decreased after PCA treatment, whereas dopamine and its major metabolite HVA remained unchanged. Further, the changes of ^{123}I-ADAM specific binding ratio in the raphe nucleus, substantia nigra, and globus pallidus could correlate with the alternation of serotonin in PCA-treated animals. The results suggest a practical use of [123]I-
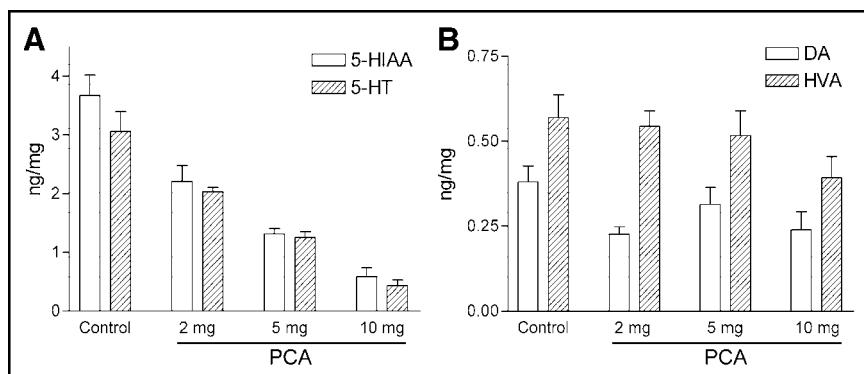

FIGURE 5. Levels of serotonin (5-HT) and 5-HIAA (A) and levels of dopamine (DA) and HVA (B) in prefrontal cortex of control and various PCA-treated rats (n = 5–8 per group).
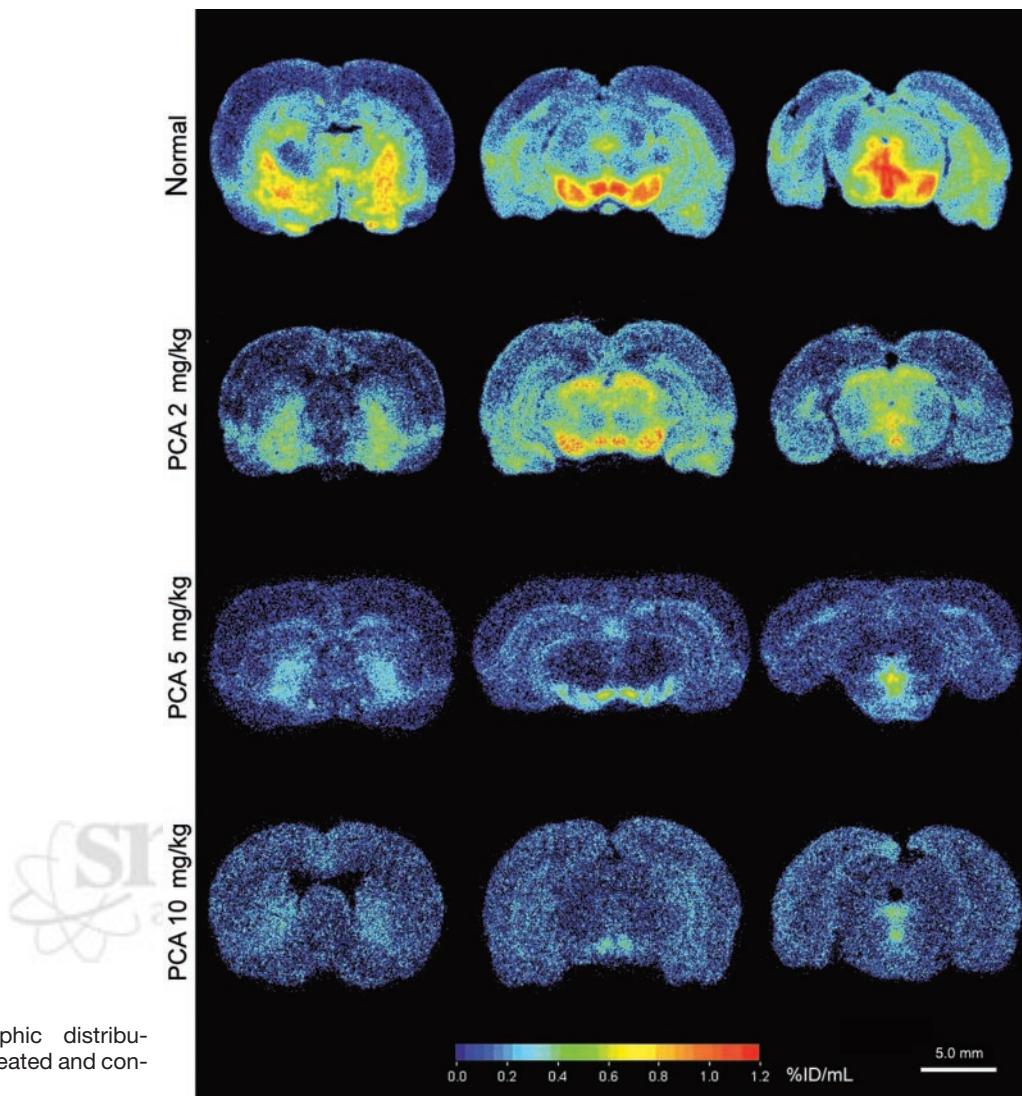
FIGURE 6. Autoradiographic distributions of ^{123}I-ADAM in PCA-treated and control (normal) rat brains.

ADAM as a valuable marker for probing serotonergic neurons as well as for quantitative functional assessment. The magnitude of change in ^{123}I-ADAM specific binding ratio was different among brain regions after low-dose PCA treatment (2 mg/kg). The greatest change was observed in the globus pallidus, followed by the substantia nigra, dorsal raphe nucleus, prefrontal cortex, and hippocamus. Less decline in ^{123}I-ADAM specific binding ratio was detected in the lateral hypothalamus, where the medial forebrain bundle lies. These differences in decline of ^{123}I-ADAM specific binding ratio may result from different vulnerability to the serotonin neurotoxin among brain regions (*18*).

At higher doses of PCA (10 mg/kg PCA-treated rats), the changes of ^{123}I-ADAM specific binding ratio in the prefrontal cortex did not match the decline of serotonin content. This phenomenon may be due to the presence of degenerating and nonfunctional serotonergic neurons with residual transporter protein. Alternatively, it may result from limited protein available in the prefrontal cortices as compared with other SERT-rich sites. At this dose of PCA treatment,

differences in the decline of the ^{123}I-ADAM specific binding ratio among brain regions were lessened due to close-to-complete loss of the serotonin neuron (*19*) though relatively high residual radioactivity (45%) was observed in the hippocampal region, suggesting a notable nonspecific binding in vivo. Similarly, Choi et al. reported a high nonspecific SERT binding (33%) in the hippocampal region by examining the in vivo drug specificity after pretreatment of selective serotonin reuptake inhibitors (*3*). We view ^{123}I-ADAM as a good serotonin marker, but its use will require careful interpretation, especially measuring SERT in the prefrontal cortex and hippocampus.

CONCLUSION

This study demonstrates that ^{123}I-ADAM rapidly penetrates the blood–brain barrier, achieving local brain concentrations compatible with its use as an in vivo imaging agent. Transient equilibrium can be achieved by 2 h after intravenous injection of the radiotracer. In addition, the regional
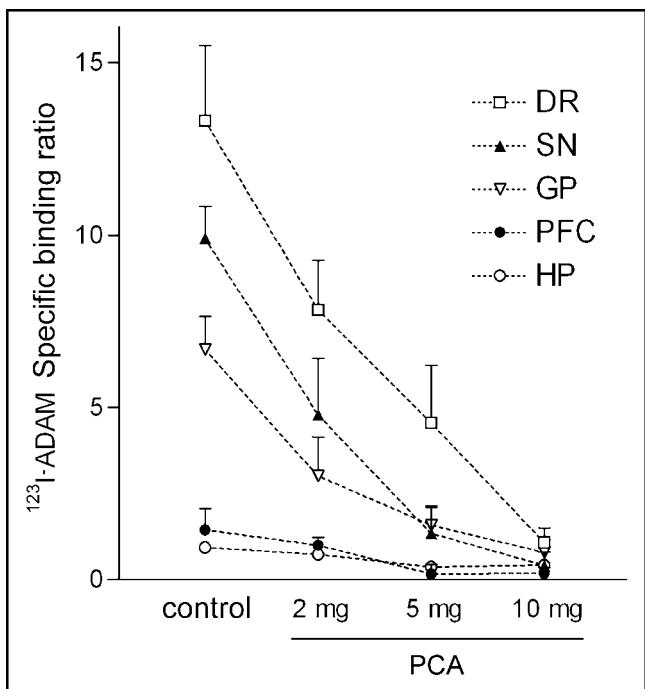
FIGURE 7. Specific binding ratio of ^{123}I-ADAM in PCA-treated and control rat brains. DR = dorsal raphe; SN = substantia nigra; GP = globus pallidus; PFC = prefrontal cortex; HP = hippocampus.

distribution of radioactivity is similar to the known distribution of SERT in both rat and mouse brains. We also showed that destruction of serotonergic neurons after treatment with PCA abolished the uptake of radioactivity into serotonergic nerve terminal-rich regions (e.g., substantia nigra, globus pallidus, and raphe nuclei). A lower specific binding ratio was noted in the sparsely innervated regions such as the prefrontal cortex. Finally, a high specific binding ratio to SERT-rich sites in vivo makes it an appropriate radiotracer for solitary studies of serotonin function in living humans.

ACKNOWLEDGMENTS

REFERENCES

1. Kasper S, Tauscher J, Willeit M, et al. Receptor and transporter imaging studies in schizophrenia, depression, bulimia and Tourette's disorder: implications for psychopharmacology. *World J Biol Psychiatry.* 2002;3:133–146.
2. Scheffel U, Dannals RF, Suehiro M, et al. Development of PET/SPECT ligands for the serotonin transporter. *NIDA Res Monogr.* 1994;138:111–130.
3. Choi SR, Hou C, Oya S, et al. Selective in vitro and in vivo binding of ^{125}I-ADAM to serotonin transporters in rat brain. *Synapse.* 2000;38:403–412.
4. Oya S, Choi SR, Hou C, et al. 2-((2-((dimethylamino)methyl)phenyl)thio)-5-iodophenylamine (ADAM): an improved serotonin transporter ligand. *Nucl Med Biol.* 2000;27:249–254.
5. Acton PD, Choi SR, Hou C, Plossl K, Kung HF. Quantification of serotonin transporters in nonhuman primates using ^{123}I-ADAM and SPECT. *J Nucl Med.* 2001;42:1556–1562.
6. Lin KJ, Ye XX, Yen TC, et al. Biodistribution study of ^{123}I-ADAM in mice: correlation with whole body autoradiography. *Nucl Med Biol.* 2002;29:643–650.
7. Kauppinen TA, Bergstrom KA, Heikman P, Hiltunen J, Ahonen AK. Biodistribution and radiation dosimetry of [^{123}I]ADAM in healthy human subjects: preliminary results. *Eur J Nucl Med Mol Imaging.* 2003;30:132–136.
8. Sur C, Betz H, Schloss P. Immunocytochemical detection of the serotonin transporter in rat brain. *Neuroscience.* 1996;73:217–231.
9. Charon Y, Laniece P, Tricoire H. Radio-imaging for quantitative autoradiography in biology. *Nucl Med Biol.* 1998;25:699–704.
10. Johnston RF, Pickett SC, Barker DL. Autoradiography using storage phosphor technology. *Electrophoresis.* 1990;11;355–360.
11. Motoji N, Hayama E, Shigematsu A. Studies on the quantitative autoradiography. I. Radioluminography for quantitative autoradiography of ^{14}C. *Biol Pharm Bull.* 1995;18:89–93.
12. Paxinos G, Watson C. *The Rat Brain in Stereotaxic Coordinates.* 4th ed. Burlington, MA: Academic Press; 1998.
13. Ishiwata K, Ogi N, Tanaka A, Senda M. Quantitative ex vivo and in vitro receptor autoradiography using ^{11}C-labeled ligands and an imaging plate: a study with a dopamine D2-like receptor ligand ^{11}C-nemonapride. *Nucl Med Biol.* 1999;26: 291–296.
14. Ichise M, Meyer JH, Yonekura Y. An introduction to PET and SPECT neuroreceptor quantification models. *J Nucl Med.* 2001;42:755–763.
15. Ramamoorthy S, Bauman AL, Moore KR, et al. Antidepressant- and cocaine-sensitive human serotonin transporter: molecular cloning, expression, and chromosomal localization. *Proc Natl Acad Sci USA.* 1993;90:2542–2546.
16. Pletscher A, Burkhard WP, Bruderer H, Gey KF. Decrease of cerebral 5-hydroxytryptamine and 5-hydroxy-indoleacetic acid by an arylalkylamine. *Life Sci.* 1963;11:828–833.
17. Vorhees CV, Schaefer GJ, Barrett RJ. *p*-Chloroamphetamine: behavioral effects of reduced cerebral serotonin in rats. *Pharmacol Biochem Behav.* 1975;3:279–284.
18. Mamounas LA, Molliver ME. Evidence for dual serotonergic projections to neocortex: axons from the dorsal and median raphe nuclei are differentially vulnerable to the neurotoxin *p*-chloroamphetamine (PCA). *Exp Neurol.* 1988; 102:23–36.
19. Fuller RW. Effects of p-chloroamphetamine on brain serotonin neurons. *Neurochem Res.* 1992;17:449–456.